

Water in Hydrogels. An NMR Study of Water/Polymer Interactions in Weakly Cross-Linked Chitosan Networks

D. Capitani,^{*†} V. Crescenzi,[‡] A. A. De Angelis,^{‡§} and A. L. Segre[†]

Institute of Nuclear Chemistry, CNR, Area della Ricerca di Roma, C.P. 10, 00016 Monterotondo Stazione, Rome, Italy; and Department of Chemistry, University of Rome "La Sapienza", P.le. A. Moro 5, 00185 Rome, Italy

Received December 11, 2000; Revised Manuscript Received March 8, 2001

ABSTRACT: A pulsed low-resolution ^1H NMR relaxation study at 75 MHz was performed on chitosan and on two lightly cross-linked chitosan networks with a different degree of cross-link and different amount of added water. The spin–lattice relaxation time T_1 , the spin–spin relaxation time T_2 , and the free induction decay (FID) were measured in the 200–320 K temperature range. An aperiodic saturation recovery sequence was applied for measuring T_1 , while a CPMG sequence was used for measuring T_2 . A full deconvolution of FIDs allows a plethora of information. Lightly cross-linked chitosan chains form super adsorbing hydrogels. The amount of water in these gels at the swelling equilibrium is so high to hide completely the properties of bound water. Thus, dried samples of chitosan and of cross-linked chitosan derivatives were partially rehydrated and studied as a function of added water and of temperature. Data obtained from a ^1H NMR relaxation study allowed us to measure the number of water molecules in different shells of solvation of macromolecules. Only about four water molecules per repeat unit are tightly coordinated by chitosan while the number of water molecules tightly coordinated markedly increases for cross-linked chitosans and is correlated with the maximum swelling properties of the networks.

Introduction

The state of water in hydrogels is a fascinating subject with theoretical and practical implications,¹ but from just a few, recent papers can a clear understanding of the phenomenon with a sharp focus on the main physical-chemical factors involved in the hydration of natural or synthetic polymers and of hydrogels be obtained.^{2–4}

Here we wish to contribute an answer to some of the questions related to the state(s) of water adsorbed by highly hydrophilic hydrogels. To this end we have considered three polymeric systems: the polysaccharide chitosan and two weakly cross-linked chitosan derivatives. The latter, prepared using 1,1,3,3-tetramethoxypropane (TMP) as cross-linking agent, were previously characterized in terms of degree of reticulation (DR), water uptake, and structure⁵ and have a DR estimated at <2% for sample S0 and DR \approx 2–3% for sample S1.

The purpose of our study is to explain the experimental observation that lightly cross-linked chitosan chains can adsorb water differently, despite their very low DR values, and in amounts distinctly higher compared to their parent polymer. At the same time, we wish to gain insight into the properties of water when bound to chains able of yielding superadsorbent networks.⁶

In aqueous media, the degree of cross-link is a structural parameter important in determining the swelling properties of a polymeric network.

To obtain a gel with an amount of water as high as possible the amount of cross-linked units must be kept as low as possible and yet able to give an insoluble polymer, i.e., a superabsorbent network.⁶ The macroscopic behavior of an hydrogel, at a different degree of

cross-linking, is obtained by measuring the swelling properties as a function of the ionic strength and pH.⁶ In turn, low-resolution NMR provides insight into the dynamics of water molecules and their environment.

The NMR characterization of polymer–water interactions cannot be done using fully swollen hydrogels.^{3, 4} In fact, the amount of free water in these systems is so high as to hide completely the NMR signals both of the polymer and of water either tightly bound to the polymer or located in an external solvation shell around the chains. However, it is possible to dehydrate the gels and to perform a subsequent rehydration with known amounts of H_2O . Measurements have been then performed as a function of temperature and of the hydration degree for each of the three systems considered.

This paper describes the NMR experimental data and the information obtainable therefrom.

In the literature it is well demonstrated that, in hydrogels, water is present in different states of solvation; however, no precise quantitative evaluation of water in different shells is given. This evaluation is one of the main purposes of our study.

Experimental Section

Materials. Chitosan and 1,1,3,3-tetramethoxypropane (TMP) were purchased from Fluka. The synthesis of chitosan/TMP hydrogels has been previously described.⁵ The reaction is sketched in Figure 1.

The molecular weight of un-cross-linked chitosan is 255 ± 1 kDa, and the degree of *N*-acetylation (DA) is $9.1 \pm 0.5\%$.⁷ Two cross-linked chitosan/TMP gels were prepared, having cross-linking degrees $S0 < 2\%$ and $S1 \approx 2–3\%$, as determined by solid-state NMR.⁵ Henceforth we denote these gels by their respective cross-linking degree, S0 and S1. Un-cross-linked chitosan is denoted as U.

Maximum Equilibrium Swelling in Water. The maximum equilibrium swelling in water S is defined as the ratio of the weight of the swollen gel at equilibrium in water over the weight of the dry polymer.

[†] Area della Ricerca di Roma.

[‡] University of Rome "La Sapienza".

[§] Present address: Department of Chemistry, University of California, Irvine, CA 92697-2025.

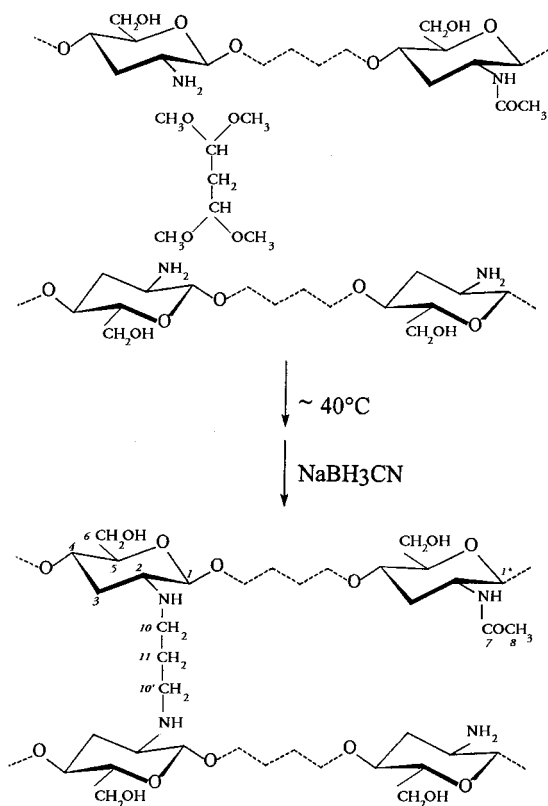


Figure 1. Chitosan and the reaction leading to the cross-linked chitosan.

Chitosan/TMP gels were extensively dialyzed against bidistilled water ($\chi = 1.3 \mu\text{S/cm}$). After wiping away excess surface water, the weight W of the gel was measured. Then the sample was freeze-dried and the weight W_d of the dry gel was measured. This procedure was repeated approximately five times for each gel. The maximum equilibrium swelling S was calculated as the average value over five measurements: $S = \Sigma(W/W_d)/5 \pm \Delta S$. The standard deviation ΔS was calculated by applying the error propagation analysis. The maximum swelling ratio was $S = 50 \pm 10$ for sample S1 (DR ≈ 2 –3%) and $S = 190 \pm 20$ for sample S0 (DR $< 2\%$), while chitosan as such does not form a transparent gel.

NMR Methods. ^{13}C CP-MAS NMR Spectra. Samples were freeze-dried. Powdered samples were packed in 4 mm zirconia rotors and sealed with Kel-F caps.

^{13}C CP-MAS NMR spectra at 50.28 MHz were obtained on a Bruker AMX-200 NMR spectrometer. The spin rate was 8 kHz, the pulse width was $3.5 \mu\text{s}$, and the contact time for the cross-polarization experiment was 1 ms. Other details of the CP-MAS spectra are given elsewhere.⁵

Samples for NMR Relaxation Measurements. After extensive dialysis, the gels were cut into small pieces and freeze-dried. A dry, white powder was obtained in all cases. A carefully controlled amount of water was added, following the same procedure for each sample. We define the ratio $W_0 = \text{mol of water added/mol of repetitive units of chitosan}$. Samples were placed in standard 5 mm NMR tubes (and sealed). The height of each sample was 0.4 cm in order to keep the samples well within the NMR coil. Samples with $W_0 = 4.6, 9.2$, and 18.0 were prepared for S0, S1 and U.

NMR Relaxation Measurements. Pulsed low-resolution ^1H NMR measurements were performed at 75 MHz on a Spinmaster spectrometer, Stelar, Mede (Pavia), Italy. A variable temperature unit (Stelar, VTC91) equipped with a standard Bruker nitrogen evaporator system or with a nitrogen flow from a pressurized line was used in the temperature range 180–320 K. The dead time of the instrument is $7 \mu\text{s}$. A variable attenuator placed between the transmitter output and the probehead, allowed to tune the 90 and 180° pulses at fixed pulse lengths, 4 and $8 \mu\text{s}$, respectively.

Free induction decays (FIDs) were measured using the 90° pulse and a proper relaxation delay (RD = 10 s) between successive scans; 16 scans and 2048 data points were collected in each experiment.

Spin-lattice relaxation times were measured by the aperiodic saturation recovery sequence⁸ (APSR). This sequence consists of a long train of 90° pulses (15 pulses in our case) spaced in an aperiodic way, i.e., decreasing the delay between pulses in a linear way. At the end of the pulse train the relaxation recovery proceeds with a variable delay t_i placed before a fixed 90° . APSR experiments were performed with a multiblock, multiscan procedure; 64 blocks, corresponding to 64 different delays t_i were collected in each experiment; each block was acquired with a size of 512 data points. To improve the signal/noise ratio, 16 scans were performed.

Spin-spin relaxation times were measured by applying the CPMG⁹ sequence. At $T = 300$ K both the CPMG and the AP-CPMG sequence¹⁰ were applied; the inter-pulse time 2τ between the 180 and 90° pulses was always kept at $100 \mu\text{s}$. Depending on the T_2 values, 1024, 2048, or 4096 different echoes were collected.

In systems with multiple T_2 relaxations, the choice of the interpulse time, 2τ , is not trivial and depends on the value of T_2 . Before performing a CPMG experiment, 2τ must be properly chosen in order to collect the highest possible number of echoes; thus, when T_2 is short also 2τ must be short. Note that errors due to the diffusion, spin-spin coupling, and chemical exchange can be reduced or eliminated from T_2 measurements by using a CPMG sequence if a sufficiently short 2τ value is chosen. However, it has been shown¹¹ that, in a very short 2τ regime, spins may not dephase significantly in the period between pulses and may be locked by the effective refocusing field of the CPMG sequence. Hence with very short 2τ values, the CPMG sequence will measure the spin-lattice relaxation time in the rotating frame $T_{1\rho}$ instead of measuring the effective T_2 . When T_2 is much shorter than $T_{1\rho}$ similar effects have been observed in solids, gels, viscous liquids and tissues.^{11,12} Thus, as $2\tau \rightarrow 0$, spin locking effects in fast CPMG sequence may lead to a marked increase in the measured transverse spin-spin relaxation time. As a consequence T_2 measured with the CPMG sequence in the short 2τ regime may be indistinguishable from $T_{1\rho}$ measured in a locking field equivalent to that one produced by the refocusing pulses. To eliminate this possibility, in all samples before measuring T_2 as a function of the temperature, preliminary measurements for evaluating the possible presence of the spin-locking effects were performed. It has been previously shown¹⁰ that these spin-locking effects can be eliminated using an alternating phase CPMG, namely, AP-CPMG, sequence:

$$(90)_x - \tau - [(180)_y - 2\tau - (180)_y - 2\tau - (180)_y - 2\tau - (180)_y - 2\tau]_n$$

At room-temperature T_2 measurements as a function of τ were performed by the CPMG method and by the AP-CPMG method. Because of weak spin-locking effects, for 2τ values ranging from 40 to $60 \mu\text{s}$, T_2 values measured applying the CPMG sequence are slightly longer than those measured when $2\tau \geq 80 \mu\text{s}$. Hence, in the full temperature range, an interpulse $2\tau = 100 \mu\text{s}$ was always used.

NMR Data Analysis. Analysis of the NMR data was performed by the program STEFIT¹³ that uses a "Simplex" algorithm for the fit of various functional forms.¹³

FIDs. Due to the presence of fast and slow relaxing components, deconvolution in the time domain of FIDs is always necessary.¹⁴

The shape of the free induction decays (FIDs) is fit to a sum of Gaussian line shapes

$$Y = C_0 + \sum_i W_i \exp[-t^2/G_i^2], \quad i = 2 \text{ or } 3 \quad (1)$$

where C_0 is the mean value of the noise, W_i is the spin density of the i component and G_i is the width of the Gaussian decay.

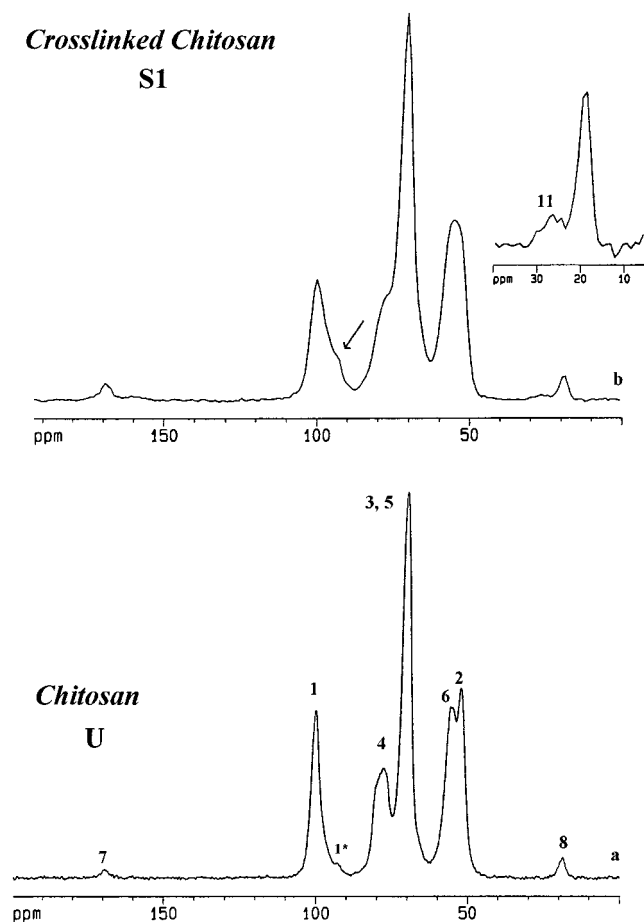


Figure 2. 50.28 MHz ^{13}C CP-MAS NMR spectra of (a) chitosan sample U and (b) a chitosan/TMP network with a low ($\approx 2\text{--}3\%$) degree of cross-linking, sample S1. In spectrum b, the arrow shows the presence of a splitting of the resonance due to the anomeric C atom, this splitting has been attributed to γ -gauche turns.⁵ In spectrum a, the small resonance marked 1* is due to the anomeric carbon atom of acetylated units well observable on the signals 7 and 8.

The second moments M_2^H of the FID were also obtained by applying the relationship $M_2^H = 2/G^2$.

Note that when more than one component is present their relative amount is proportional to their spin density, which is calculated as the origin intercept of each component of the FID.⁸ Thus, for all components, we fully define the FID when we can give its second moment and the relative spin density.

T_2 Relaxation Data Analysis. CPMG and AP-CPMG experiments lead to exponential or multiexponential decays

$$Y = C_0 + \sum_i W_i \exp[-t/T_{2i}], \quad i = \text{number of components} \quad (2)$$

where again C_0 is the mean value of the noise, W_i is the spin density of the i component and T_{2i} is the spin-spin relaxation time of the i component.

Note that by use of specific sequences making use of echoes, T_2 can be directly measured only on sufficiently narrow NMR lines. Thus, this measurement is relevant for the water component only.

T_2 is a monotonic function of the correlation time τ_c ; thus the shorter is the T_2 value, the stiffer is the system. Typical values are 1–2 s for liquids, 10^{-2} – 10^{-3} s for macromolecular systems in solution, and 10^{-5} – 10^{-6} s for solids.

T_1 Relaxation Data Analysis. The analysis of T_1 relaxation data of hydrogels can be cumbersome. As previously observed, in cross-linked networks with added water, due to different T_2 relaxation times, two or three Gaussian functions were used for obtaining the FID shape. As a matter of fact, in

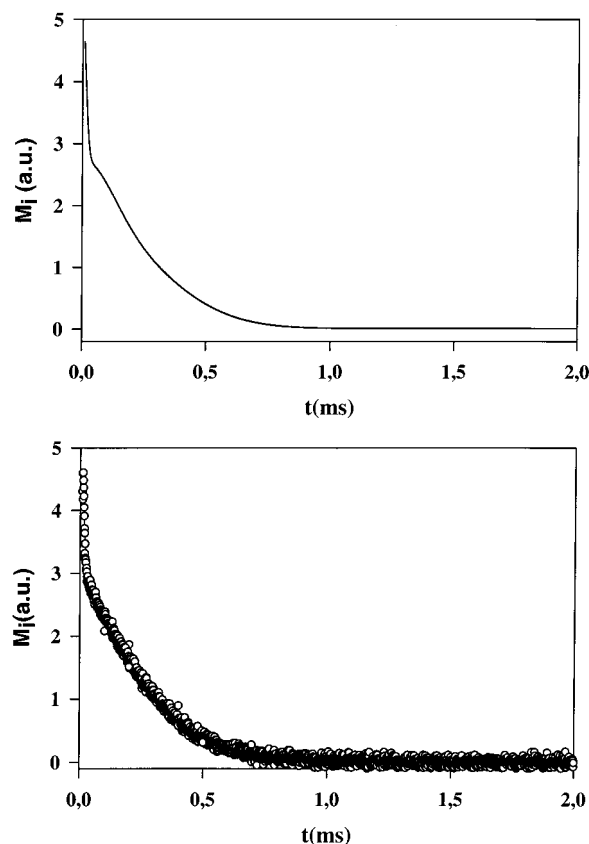


Figure 3. FID of polymer U (un-cross-linked chitosan) with $W_0 = 4.6$ ($W_0 = [\text{H}_2\text{O}]/[\text{repetitive unit}]$): bottom, experimental FID; top, simulation with three Gaussian components. The amount of water, equivalent to the spin density, is obtained from the origin intercept of each component.

an APSR multiblock experiment, each experiment leads to an FID obtained with the proper time increment τ_i , with $i = 1, \dots, M$ and $M = \text{number of blocks}$. As a function of the time increment, the intensity of these FIDs increases. As shown in Figure 3, at least two components are clearly observed in each FID of an APSR experiment. Let us label as A the fast T_2 relaxing component and B the slow T_2 relaxing component.

Following a method previously outlined¹⁴ we can cut each FID after a suitable initial delay. In this way we obtain the T_1 value of the long T_2 relaxing component, T_{1B} according to

$$I_{Bi} = B_0 + B \exp(-\tau_i/T_{1B})$$

For obtaining the T_1 value of the short T_2 relaxing component, T_{1A} , a full best fit of all M different FIDs is necessary. In fact for the evaluation of T_{1A} it is necessary to best fit all other components $I_{Ai} = I_{Ti} - I_{Bi}$, with $i = 1, \dots, M$.

Thus, from this best fit we obtain all M spin densities I_{Ai} and finally T_{1A} .

In all our samples, all spin lattice relaxation times respectively due to the fast and to the slow T_2 relaxing component, are equal within the experimental error, thus showing that a strong spin diffusion process is active on a spin-lattice time scale.

Confidence Intervals and Errors. From a previous analysis, we obtain best fitted functions (FID's, T_1 , T_2) which are accepted with a confidence better than 95%. Estimated errors are better than 5% of the nominal value for G_i and T_{2i} and better than 10% of the nominal value for T_{1i} , and for all populations $W_{a,b,c}$. Estimated errors are on the order of 20% for second moments.

Generality on Water in Hydrogels. Different states of the water in hydrogels are characterized by different correlation times,¹⁵ which, in the absence of strong exchange, cause the onset of different transversal relaxation times. Because

of the presence of different local mobility, i.e., when the chemical exchange is ineffective, different transverse relaxation times are observable. Thus, as previously observed¹⁴ the spin diffusion process is inactive on a T_2 time scale.

¹H NMR relaxation times (T_1 , T_2 , $T_{1\rho}$) provide insight into the dynamics of water molecules and their local environment.¹⁴ The general feature of the hydration layer in hydrophilic macromolecular systems is the distribution of correlation times resulting in a distribution of the transverse relaxation times. For the transverse relaxation mechanism, the dominant process is the chemical exchange between water protons and exchangeable protons of chitosan, whereas spin diffusion equalizes the longitudinal relaxation in hydrated polymers.

As a function of the temperature the different components of T_2 are characterized by the presence of maxima and minima due to the passage of water from one solvation shell to another one.¹⁶ Derbyshire first proposed a simple treatment of relaxation times on hydrated systems on this basis.²

Another way of treating the presence of maxima and minima on transversal relaxation rates of hydrated polymers is to admit that many water fractions exist, differently bound, with variable populations as a function of the temperature. This point of view was amply discussed by McBrierty^{3,4} who treats the various solvation shells separately and the water as acting as a plasticizer or an antiplasticizer.

Results and Discussion

Dried Polymers. Following a previously proposed method,³ to achieve a better interpretation of the hydrated systems, examination of the dry samples was first carried out. The cross-linked polymers S0 and S1 are compared to un-cross-linked chitosan, labeled U.

Let us consider the simplest possible NMR experiment, i.e., the FID, performed as a function of the temperature on dried samples. In all samples, a close inspection of the FID experiment reveals the presence of two components, a fast relaxing one attributed to the polymer lattice and a slow relaxing one, much weaker, which we think is due to the presence of acetyl groups.¹⁴ The spin density of this component is quite low in all samples. To have a better fit of the data, we introduced the presence of these acetylated groups in the data analysis; however, their presence will not be further discussed.

At room temperature the second moment¹⁴ of un-cross-linked chitosan U is about $1 \times \exp 10^{10} \text{ s}^{-2}$, exactly as in samples S1 and S0. For all samples, decreasing the temperature, only a modest increase of second moments is observable. Since the second moment of an NMR line is, within a first approximation, proportional to the stiffness of the material,¹⁸ from our data, we may conclude that the stiffness of all dried samples is about the same. T_1 data on dried samples confirm the above result.

In the dry cross-linked chitosan, a conformational variation occurs, quite well observable with CP-MAS techniques (see Figure 2) and previously discussed.⁵ This conformational variation of the polymer may act in such a way to expose -OH functions to solvent, easing in this way the water-macromolecule binding.

Rehydrated Polymers. To gain information on polymer-water interactions, a careful NMR study was performed on partially rehydrated samples of U, S1, and S0. The basic term for the comparison is a sample of un-cross-linked chitosan (U) to which a very small amount of water was added. Let us consider the FIDs of rehydrated samples of U with amounts of added water

corresponding to the molar ratios:

$$W_0 = 4.6, W_0 = 9.2, \text{ and } W_0 = 18.0, \text{ with } W_0 = \frac{[\text{H}_2\text{O}]}{[\text{repeating monomer}]}$$

A careful analysis of FIDs for $W_0 = 4.6$ shows the presence of at least three Gaussian components; see Figure 3. Again, for $W_0 = 9.2$ and $W_0 = 18.0$ all FIDs can be simulated with three Gaussian components. As a function of the temperature, we can plot the normalized spin density value of the more rigid component, i.e., of the component characterized by the higher value of the second moment; see Figure 4.

With regard to the rigid component (fast decaying) of the FID, it must be noted that a net increase of its spin density is observed when a fraction of the gel freezes. This effect can be observed clearly near the melting point of an included solvent in the presence of its free state.¹⁹

Thus, near 270 K, when free water is present, we should observe a net increase of the spin density of the stiffest component. Thus, at the same temperature, near 270 K, the spin density of the FID component due to free water goes to zero.

In Figure 4, we show the relative (normalized) spin density values for the stiff component. It must be noted that while only one Gaussian component accounts for the observed FID of the dried polymer, when water is added, for all W_0 values, three components are clearly observable in the FID.

According to current literature,^{20,21} we may interpret these multiple components as due to the macromolecule with its exchangeable groups (hydroxyl) and probably water in the first solvation shell, the second component as due to water in a second solvation shell and the third component, corresponding to the narrowest Gaussian, to "free" water in exchange with bound water.

If we plot the normalized spin density of the fastest relaxing component vs temperature, we clearly observe a transition near 270 K; see Figure 4, parts a-c.

This transition, barely observable in the sample with $W_0 = 4.6$, is very strong in samples with $W_0 = 9.2$ and 18.0. A possible interpretation of the data is that only about three to four water molecules per repeating unit are tightly coordinated to chitosan U; thus, their melting point is very low and they behave as a true solvation water. The other two components, due to "free" water and to water in the external solvation shell, freeze at a temperature barely lower than that of free distilled water, and their binding to the macromolecule is rather weak.

Let us consider the set of data obtainable from the FIDs of samples S1 and S0, recalling that in the absence of added water all FIDs of samples U, S1, and S0 are indistinguishable at all temperatures.

Let us consider the behavior of the FIDs of sample S1 when we add water, with $W_0 = 4.6, 9.2, 18.0$. Again, as in sample U, three Gaussian components are necessary to simulate the FIDs. As a function of the temperature we can plot the spin density of the more rigid component, i.e., of the component characterized by the higher value of the second moment; see Figure 4, parts d-f. In Figure 4e, at $W_0 = 9.2$ the observed transition around 260 K is quite modest, and only when $W_0 = 18.0$ (see Figure 4f) is a net transition observable near 260 K with a strong variation in the spin density of the rigid component. A possible interpretation of these data is

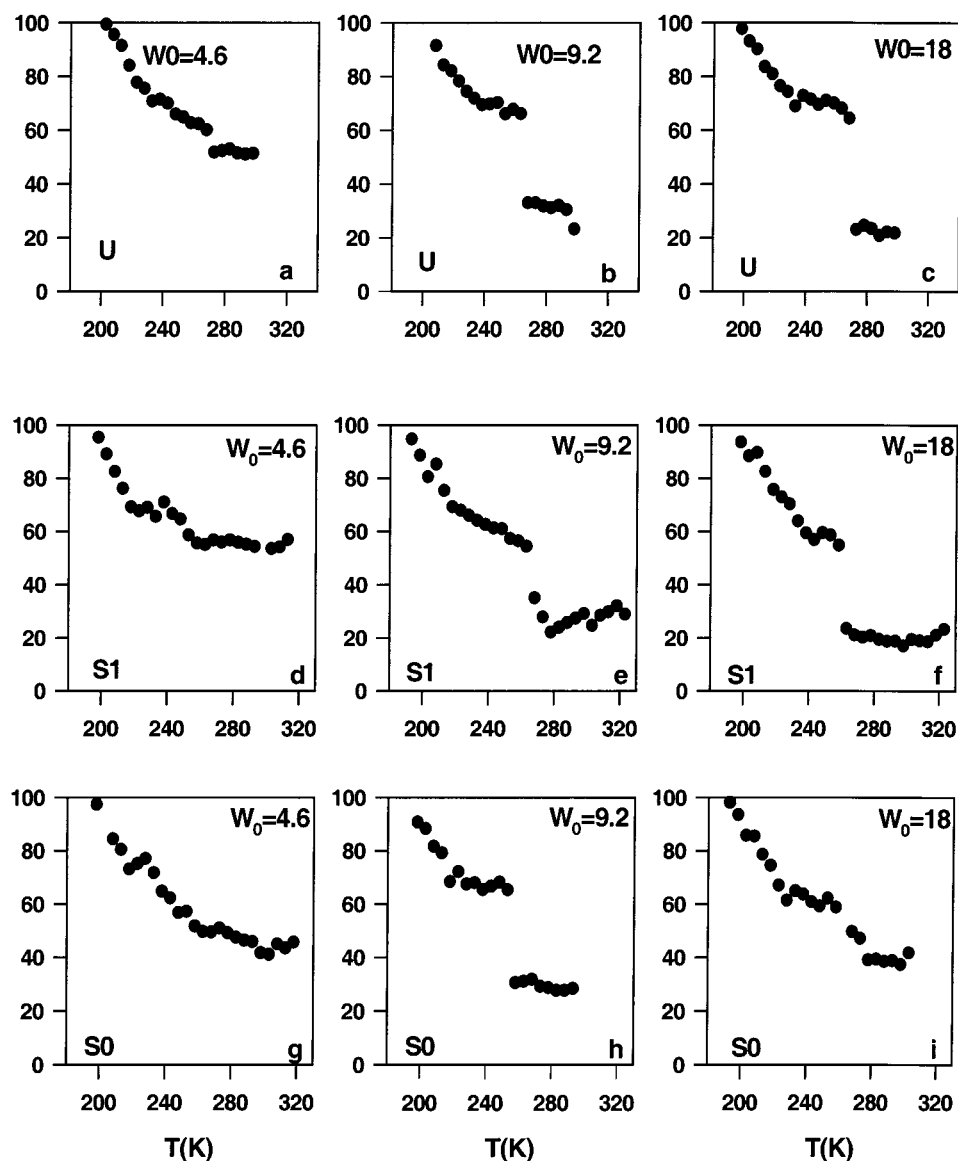


Figure 4. Normalized spin-density of the fastest relaxing Gaussian component as a function of the temperature. Polymer U, un-cross-linked chitosan, with $W_0 = 4.6$ (a), 9.2 (b), and 18.0 (c). The modest transition barely observable at $W_0 = 4.6$ shows that about 4 water molecules per residue are strictly bound. Cross-linked polymer S1 (2–3% cross-linking deg.) with $W_0 = 4.6$ (d), $W_0 = 9.2$ (e), and $W_0 = 18.0$ (f). The broad transition at $W_0 = 9.2$ shows that about nine water molecules per residue are tightly coordinated. Weakly cross-linked polymer S0 (<2% cross-linking degree) with $W_0 = 4.6$ (g), $W_0 = 9.2$ (h), and $W_0 = 18.0$ (i). At $W_0 = 9.2$ a strong secondary transition is observable at about 250 K. No transition due to free water is observable, meaning that at least 15–18 water molecules per residue are tightly bound.

that polymer S1 is able to *tightly coordinate at least eight to nine water molecules per repeating unit and that even in the presence of a relatively high amount of water, corresponding to $W_0 = 18.0$, no free water is present.*

To support this observation, we observe that in polymer S1 with $W_0 = 9.2$ the Gaussian component attributable to free water in exchange with bound water (component with the longest T_2 value), decreases in a very slow progressive way starting from 270 K and fully disappearing only at a temperature as low as 200 K, see Figure 5b.

In sample S1, at $W_0 = 18.0$, a clear transition at 260 K is observable; see Figures 4f and 5c.

Let us consider the same type of data for sample S0, following the spin densities of different components as a function of the temperature for different W_0 .

As a function of the temperature we can plot the spin density value of the more rigid component, i.e., of the

component characterized by the higher value of the second moment and the lowest T_2 ; see Figure 4, parts g–i.

Here data appear extremely regular and well clear. For $W_0 = 4.6$, a monotonic increase of the stiff component is observed. When $W_0 = 9.2$, a clear transition appears at 250 K, temperature at which all freezing water is fully bound. While for $W_0 = 18.0$ a smooth, barely observable transition appears at temperatures near to 265 K.

A possible interpretation of these data is that polymer S0 is able to *tightly coordinate about 15–18 water molecules per repeating unit.*

This observation is supported by the data reported in Figure 5, parts d–f, showing the population of the FID component characterized by the longer transversal relaxation, i.e., the water component as a function of the temperature, for S0 at $W_0 = 4.6$, 9.2, and 18.0,

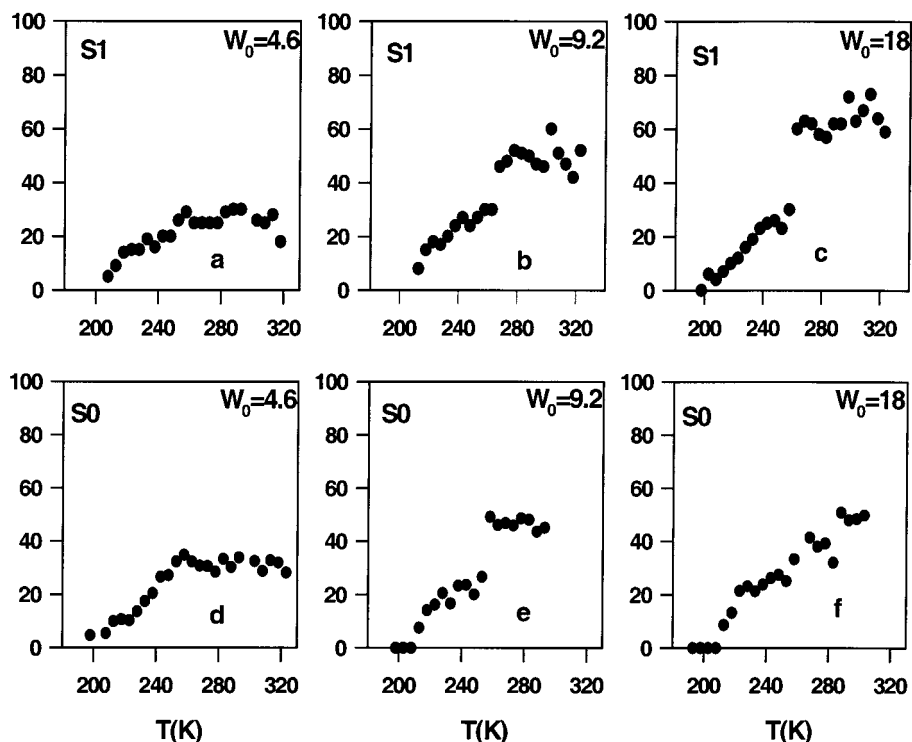


Figure 5. Normalized spin density of the FID component with the longer T_2 ; this component is due to free water in exchange with bound water. Cross-linked polymer S1 (2–3% cross-linking degree) with $W_0 = 4.6$ (a), $W_0 = 9.2$ (b), and $W_0 = 18.0$ (c). This component decreases in a very slow progressive way starting from 270 K and fully disappearing only at about 200 K. Weakly cross-linked polymer S0, with $W_0 = 4.6$ (d), $W_0 = 9.2$ (e), and $W_0 = 18.0$ (f). A strong secondary transition is well observable in part e. At least 15–18 water molecules per residue are strictly bound to the polymer since, even with $W_0 = 18.0$, no free water melting around 270 K is observable.

respectively. In Figure 5d, $W_0 = 4.6$, it is easy to see that this component decreases in a continuous way as the temperature decreases from room temperature to 200 K. A transition, possibly due to water moving from one shell of solvation to another is observable in Figure 5e, at $W_0 = 9.2$. However, the presence of a smooth transition near 260 K can be observed when $W_0 = 18.0$; see Figure 5f.

T_2 Measurements. To gain a better insight into this weakly coordinated water, a series of T_2 measurement was performed on all samples, i.e., U, S1, and S0, with different W_0 values, i.e., $W_0 = 4.6, 9.2, 18.0$, from room temperature down to about 200 K. It must be noted that a T_2 measurement performed with any echo train⁹ is efficient only along intrinsically narrow lines. Thus, when we perform a T_2 measurement on a system such as the rehydrated hydrogel, the T_2 measurement will be relevant only to the water component, and we will ignore completely the component relative to the macromolecule and to the first shell of solvated water.

As previously mentioned, regarding the general theory on the interpretation of T_2 data in hydrogels, by lowering the temperature, T_2 will decrease in any material. However in hydrated systems having many FID components, this is not always true and flat minima or apparent maxima can be found.^{2,3,4} The reason for this apparently anomalous behavior was initially identified by Derbyshire.² In fact, as a function of temperature, water can move from one solvation shell to another or even demix, causing the onset of variable amounts of free water characterized by long T_2 values.

The first observation is that, in sample U, for $W_0 = 4.6$ only one T_2 value is present (with another component whose maximum normalized spin density is about

10%) but when $W_0 = 9.2$ or 18.0 many T_2 values are measurable. The shortest T_2 component at $W_0 = 4.6$ (a), 9.2 (b), and 18 (c) is reported in Figure 6, parts a–c as a function of temperature. In Figure 7, parts a–c and Figure 8, parts a–c we report the T_2 values for each component measured in sample U with $W_0 = 9.2$ and 18.0, respectively. In Figures 7 and 8, the full circles represent the values of the T_2 components, while the empty circles show their normalized spin-densities.

In Figure 6a, an apparent maximum is observable, ascribed to the presence of a demixing. Thus, water moves from one solvation shell to another as a function of the temperature. This effect is still evident but smaller in Figure 6b and even less clear in Figure 6c, where only a discontinuity in the decreasing curve seems present. In agreement with the interpretation given for FID data, we think that this apparently monotonic behavior is mostly due to the large amount of free water present in this sample.

It must be noted that the decay obtained in a CPMG experiment is almost monoexponential in sample U when the water content is $W_0 = 4.6$. In turn, at $W_0 = 9.2$ and $W_0 = 18$, cross-linked and not cross-linked chitosan show a very different T_2 behavior. In cross-linked chitosan, the echo train obtained applying the CPMG sequence fits with a single-exponential decay. As a consequence, a single T_2 value is obtained. In turn, in not cross-linked chitosan, a three exponential decay fits with the CPMG echo train, pointing the presence of three T_2 values

Two processes tend to equalize relaxation values; these are the chemical exchange and the spin diffusion.^{14,22} Following the McBrierty treatment of spin diffusion, when we observe different T_2 values all

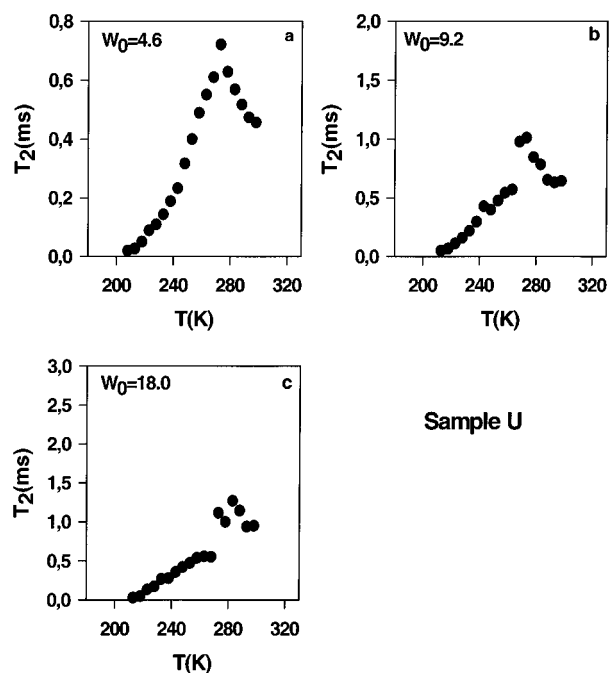


Figure 6. T_2 relaxation of sample U with $W_0 = 4.6$ (a), $W_0 = 9.2$ (b), and $W_0 = 18.0$ (c). A multicomponent behavior is observed. As a function of the temperature the fastest relaxing component of T_2 is reported. Note the presence of the singular point near 270 K even in the sample with $W_0 = 4.6$. The singularity is attributable to demixing and the presence of free water.^{2,3}

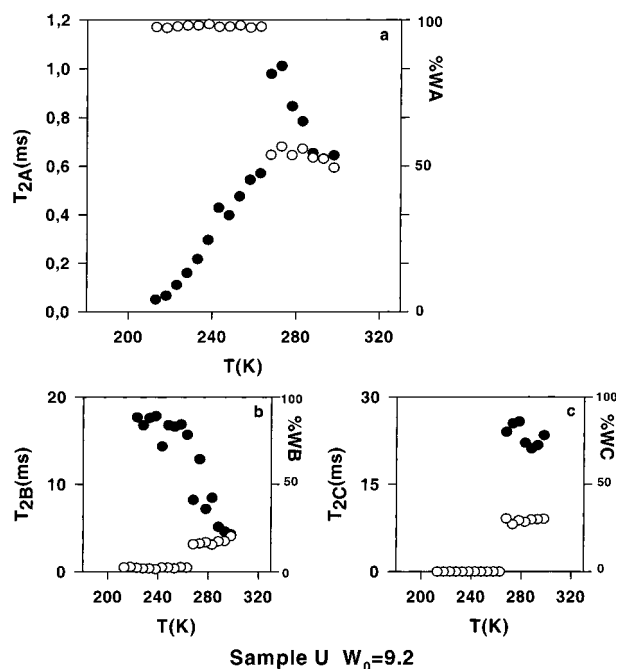


Figure 7. Spin-spin relaxation, T_2 , as a function of the temperature, in sample U with $W_0 = 9.2$: (a) fastest component. The full icons denote the T_2 values while the empty icons denote the normalized spin density. The other T_2 components are shown in parts b and c with the same notation.

present in the water component, we can conclude that this water is partitioned into microenvironments large enough to cause an inefficient spin diffusion process on a spin-spin relaxation time scale. In other words, the system presents microheterogeneity.²³

An analysis of the spin densities of these 3 components reveals that at $W_0 = 9.2$ and 18 two of these

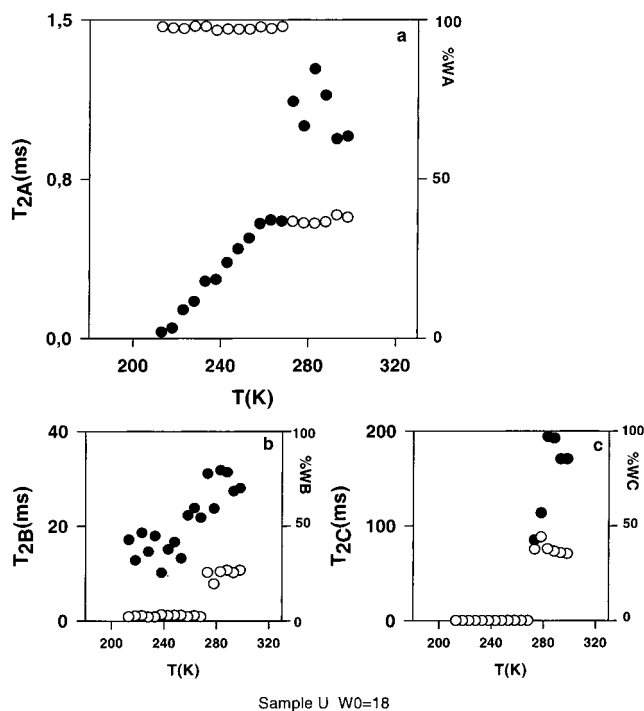


Figure 8. T_2 as a function of the temperature in sample U with $W_0 = 18.0$: (a) fastest component. The full icons denote the T_2 values, while the normalized spin density is shown as empty icons. Values relative to the other T_2 components are given in parts b and c with the same notation.

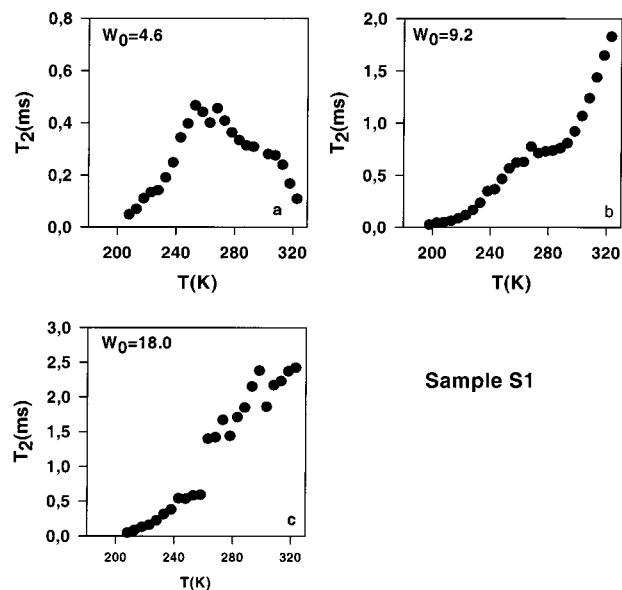


Figure 9. Sample S1 (2–3% cross-linking degree). T_2 as a function of temperature, at different W_0 . $W_0 = 4.6$ (a); $W_0 = 9.2$ (b); $W_0 = 18.0$ (c). The T_2 decay is monoexponential.

components disappear at about 270 K, so that they are effectively due to free water; see Figures 7 and 8.

Thus, T_2 data clearly support the picture of few water molecules tightly bound to chitosan and to the presence of microheterogeneity present when W_0 increases.

In Figures 9 and 10, we can observe a plot of T_2 values as a function of the temperature for rehydrated samples S1 and S0, respectively. The most relevant point is that the response of the spin system to the CPMG sequence is a monoexponential decay. Hence, by addition of water to cross-linked polymers S0 and S1, only one type of water can be observed and the water-polymer system

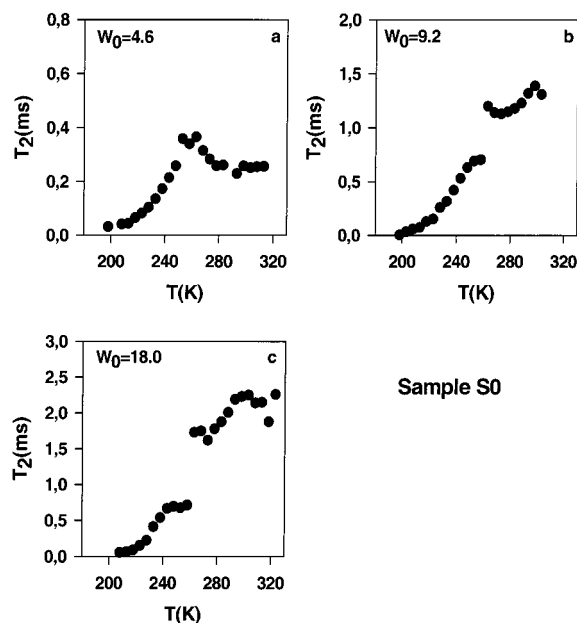


Figure 10. Sample S0 (<2% cross-linking degree). T_2 as a function of temperature, at different W_0 . $W_0 = 4.6$ (a); $W_0 = 9.2$ (b); $W_0 = 18$ (c).

appears to be homogeneous. In both S0 and S1 polymers at $W_0 = 4.6$, this added water is tightly bound; in fact the spin–spin relaxation time is rather short, with values always inferior to 0.5 ms. For $W_0 = 9.2$ and 18.0, much longer T_2 values have been observed in both polymers, to a maximum value of about 2 ms. A large number of transitions can be observed, being one of these near to the free water melting point. In this case, as for methyl acrylates, the solvent may act as a plasticizer or as an antiplasticizer according to the amount of water and to the temperature.^{3,4} However, no heterogeneity is ever present.

This means that, prior to the gel formation, rehydrated solutions of cross-linked chitosan are able to form a continuum with water.

As previously observed, water may act as a plasticizer or an antiplasticizer as a function of the concentration and of the temperature. Thus, small local transitions can be observed regarding the binding polymer–water or the number of coordinated water molecules in each solvation shell. In this way, we can rationalize a large number of small transitions observable in the relaxation vs temperature plots.

Conclusion

The main observation of this study is that water in un-cross-linked chitosan gives rise to a microheterogeneous system with domains rich of polymer and water in many solvation shells.

In turn, water in cross-linked chitosan gives rise to a continuum in which the water component appears to be tightly bound to the polymer.

NMR relaxation data from hydrogels prepared from polymers with a different cross-linking degree appear rather similar; however, the number of water molecules coordinated by S0 is higher than the corresponding number for S1. This observation agrees with the superior capability of cross-linked networks with a very low cross-linking degree to retain water, forming, eventually, fully swollen hydrogels.

Most theoretical models^{22,23} of hydrogels regard the diffusion models both for homogeneous and heterogeneous systems; however, a clear distinction between homogeneous and heterogeneous systems is present only on a gross scale, in terms of transparency. We hope that our relaxation study may partly fill this gap and that it might give a contribution to the definition of homogeneity or heterogeneity in hydrogels prior to the formation of the gel itself.

Acknowledgment. This work was financially supported by an “Ateneo grant” provided to V.C. by the University of Rome “La Sapienza”, Rome, Italy.

References and Notes

- (1) *Water in Polymers*; Rowlands, S. P., Ed.; ACS Symposium Series 127; American Chemical Society: Washington, DC, 1980.
- (2) Lewis, G. P.; Derbyshire, W.; Ablett, S.; Lillford, P. J.; Norton, S. *Carbohydr. Res.* **1987**, *160*, 397. Ablett, S.; Lillford, P. J.; Baghdadi, S. M.; Derbyshire, W. J. *Colloid Interface Sci.* **1978**, *67*, 355.
- (3) Quinn, F. X.; Kampff, E.; Smyth, G.; McBrierty, V. *Macromolecules* **1988**, *21*, 3191.
- (4) Smyth, G.; Quinn, F. X.; McBrierty, V. *Macromolecules* **1988**, *21*, 3198.
- (5) Capitani, D.; De Angelis, A. A.; Crescenzi, V.; Masci, G.; Segre, A. L. *Carbohydr. Polym.* **2001**, *45*(3), 245. Crescenzi, V.; De Angelis, A. A. In *Chitin Handbook*; Muzzarelli, A. A., Peter, M. G., Eds.; European Chitin Society: 1997; pp 415–422.
- (6) Brondsted, H.; Kopacek, J. *Polyelectrolyte gels*; ACS Symposium Series 480; American Chemical Society: Washington, DC, 1992; pp 285–304. *Superabsorbent Polymers: Science and Technology*; Buchholz, F. L., Peppas, N. A., Ed.; ACS Symposium Series 573; American Chemical Society: Washington, DC, 1994.
- (7) De Angelis, A. A.; Capitani, D.; Crescenzi, V. *Macromolecules* **1998**, *31*, 1595.
- (8) Fukushima, E.; Roeder, S. B. W. *Experimental Pulse NMR. A Nuts and Bolts Approach*; Addison-Wesley: Reading, MA, 1981; Chapter 3. Capitani, D.; Segre, A. L.; Pentimalli, M.; Ragni, P.; Ferrando, A.; Castellani, L.; Blicharski, J. S. *Macromolecules* **1998**, *31*, 3088.
- (9) Meiboom, S.; Gill, D. *Rev. Sci. Instrum.* **1958**, *29*, 688.
- (10) Suh, B. J.; Borsa, F.; Torgeson, D. R. *J. Magn. Reson.* **1994**, *A110*, 58–61.
- (11) Santyr, G. E.; Henkelman, M.; Bronskill, M. J. *J. Magn. Reson.* **1988**, *79*, 28.
- (12) Kurland, R. J.; Ngo, F. Q. H. *J. Magn. Reson.* **1986**, *73*, 425.
- (13) Sykora, S. *Program STEFIT*, part of Spinmaster software; In *Numerical Recipes. The art of Scientific Computing*; Press, W. H., Teukolsky, S. A., Flannery, B. P., Vetterling, W. T., Eds.; Cambridge University Press: Cambridge, England, 1988.
- (14) McBrierty, V. J.; Packer, K. J. *Nuclear Magnetic Resonance in Solid Polymers*; Cambridge University Press: Cambridge, England, 1993.
- (15) Müller-Plathe, F. *Macromolecules* **1998**, *31*, 6721.
- (16) Note: For the interpretation of relaxation times we will follow the simplest model of fast exchange of water molecules between a bound and an unbound state,¹⁷ $R_1 = p_f R_f + p_b R_b$, $l = 1, 2$, where $R_l = 1/T_l$ is the mean relaxation rate, R_f and R_b are the intrinsic relaxation rates of unbound and bound water, respectively, and p_f and p_b are the water fractions of the unbound and bound water compartments, respectively. Defining N_b the number of bound water molecules per sugar residue and N_M the number of sugar rings per water molecule, the previous relation can be rewritten as $R_1 = N_b R_b N_M + R_f$. Therefore if only a single bound fraction and a single unbound fraction of water molecules are present, R_1 is a linear function of N_M with a slope $N_b R_b$. We see that if N_b changes as a function of the temperature, the relaxation rate will become anomalous; as a function of the temperature, we may even obtain functions in which maxima and minima are present.
- (17) Lusse, S.; Arnold, K. *Macromolecules* **1998**, *31*, 6891.
- (18) Baley, R. T.; North, A. M.; Pathrick, R. A. *Molecular Motion in High Polymers*; Oxford Univ. Press: Oxford, England, 1981; Chapter 9.

- (19) Awaschalon, D. D.; Warnock, J. *Phys. Rev.* **1987**, *B35*, 6779.
- Warnock, J.; Awaschalon, D. D.; Schaefer, M. W. *Phys. Rev. Lett.* **1996**, *57*, 1753.
- (20) Overloop, K.; Van Gerven, L. *J. Magn. Reson.* **1993**, *A 101*, 147.
- (21) Vackier, M. C.; Hills, B. P.; Rutledge, D. N. *J. Magn. Reson.* **1999**, *138*, 36.
- (22) Packer, K. J. *Philos. Trans. R. Soc. London* **1977**, *B 278*, 59.
- (23) Amsden, B. *Macromolecules* **1998**, *31*, 8382 and references quoted therein.

MA002109X